Supporting Information

Switching water splitting photoredox preference by geometric modulation of charge consumption sites in Bi_4TaO_8Cl single crystals

Xiaolei Zhang[a], Chaofan Yuan[a], Yihe Zhang[a], Hongwei Huang[a,*], Na Tian[a,*]

[a]Engineering Research Center of Ministry of Education for Geological Carbon Storage and Low Carbon Utilization of Resources, Beijing Key Laboratory of Materials Utilization of Nonmetallic Minerals and Solid Wastes, National Laboratory of Mineral Materials, School of Materials Science and Technology, China University of Geosciences (Beijing), Beijing 100083, China

[*]Corresponding author: hhw@cugb.edu.cn (H.W. Huang); tianna65@cugb.edu.cn (N. Tian

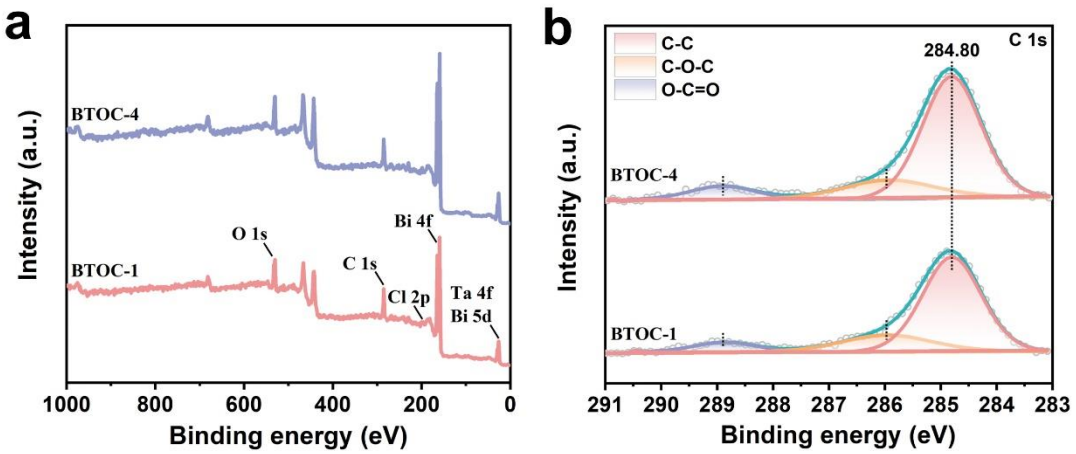

Fig. S1. (a) XPS survey spectra, and (b) high-resolution C 1s spectra of BTOC-1 and BTOC-4.

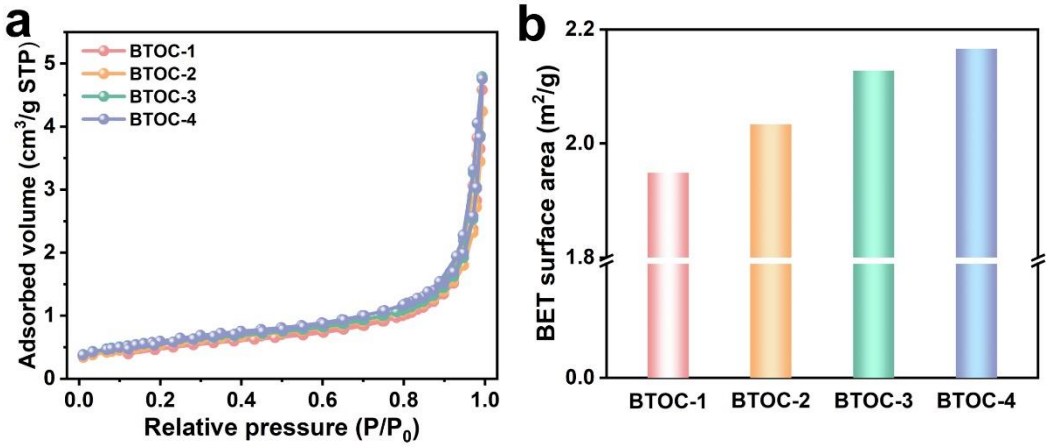

Fig. S2. (a) N_2 adsorption-desorption isothermal curves, and (b) corresponding specific surface areas of as-prepared samples.

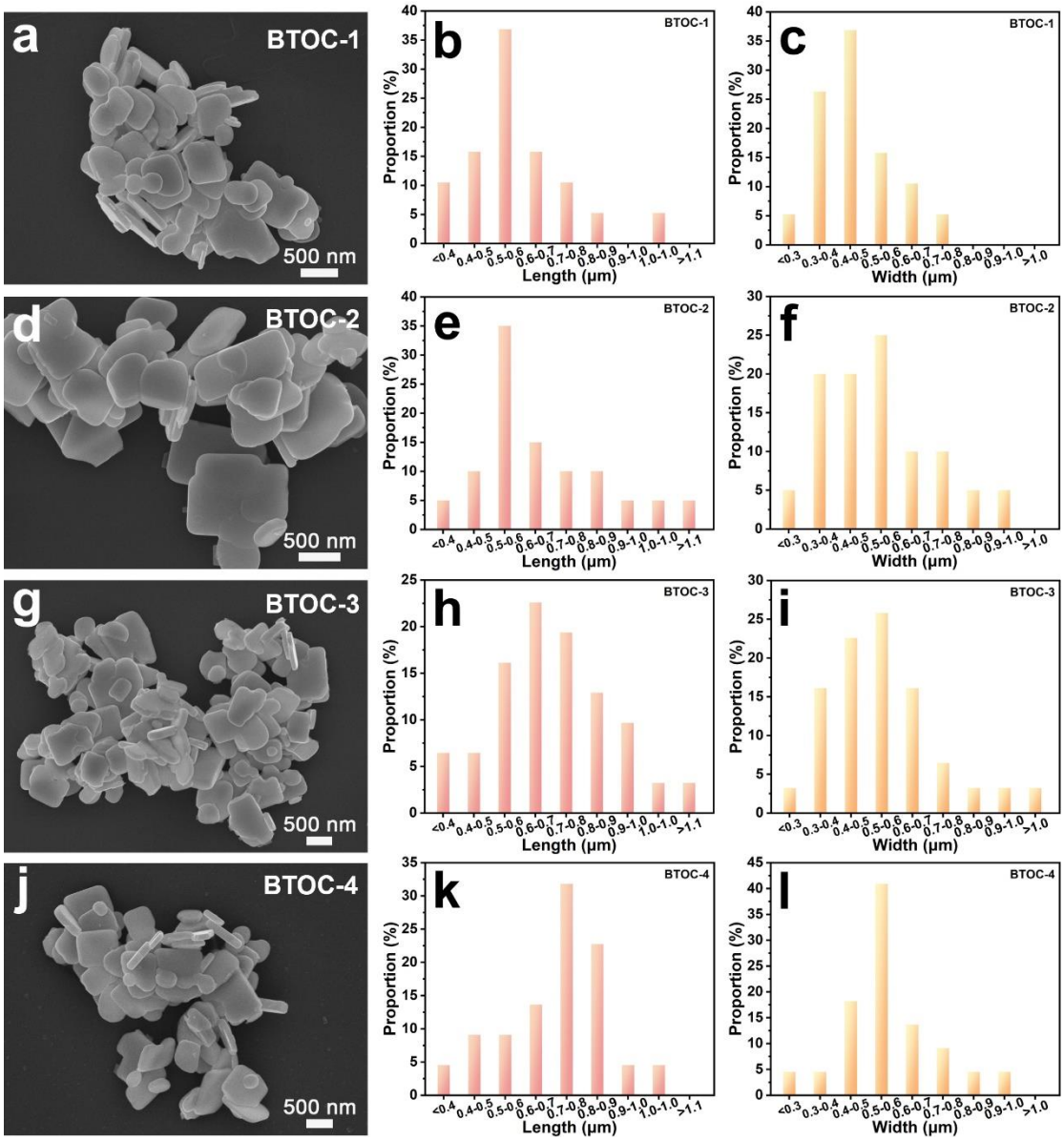

Fig. S3. Representative large-scale SEM images employed for particle size statistics, and corresponding particle size distributions of as-synthesized catalysts.

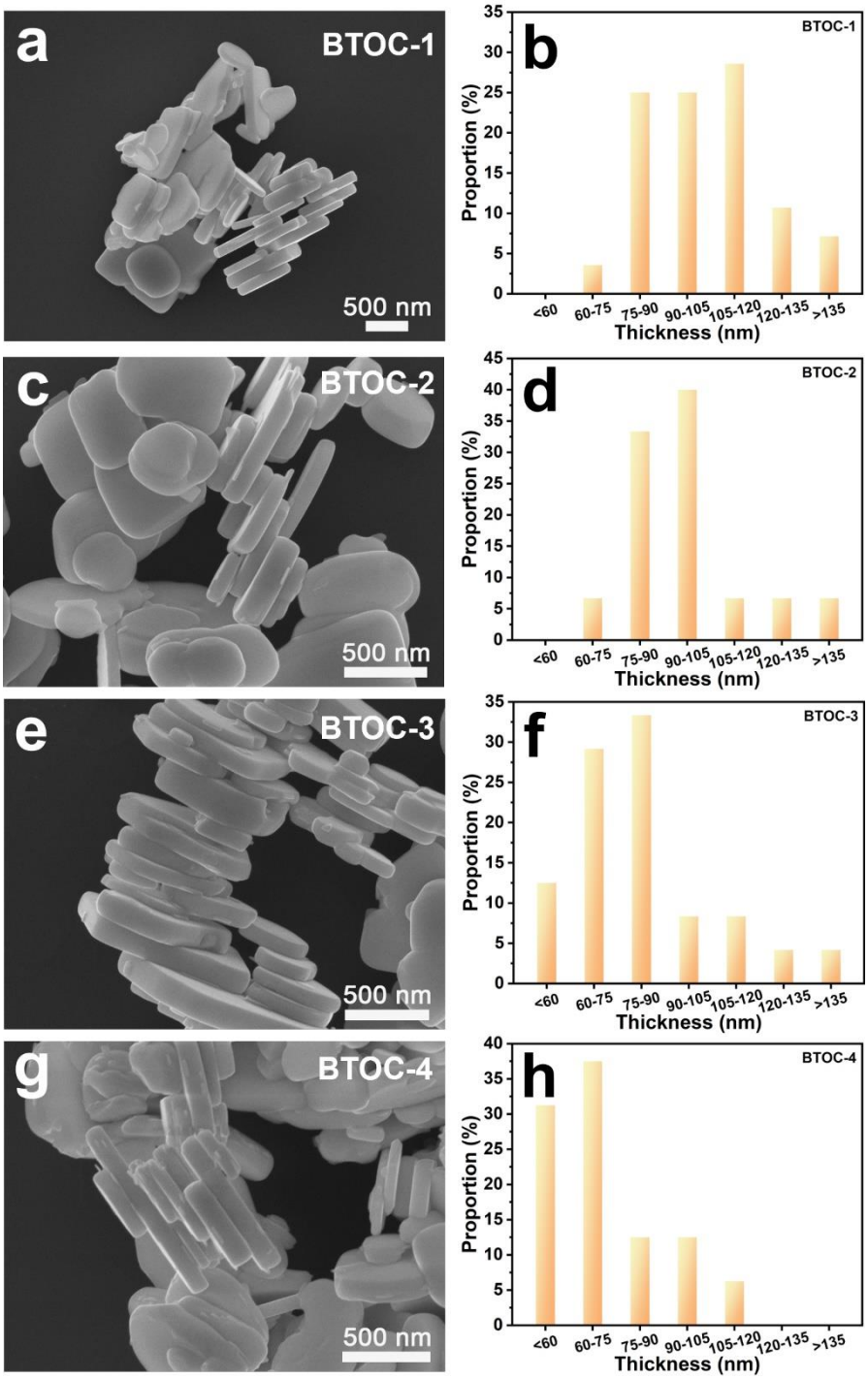

Fig. S4. Representative large-scale SEM images employed for thickness statistics, and corresponding thickness distributions of as-synthesized catalysts.

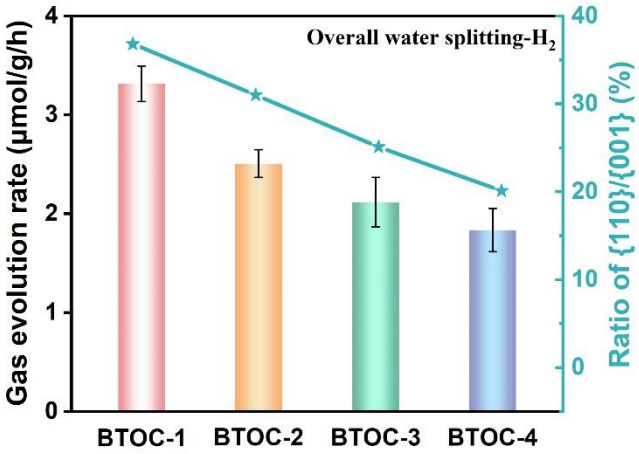

Fig. S5. Photocatalytic overall water splitting performance and the ratio of {110}/{001} for different samples.

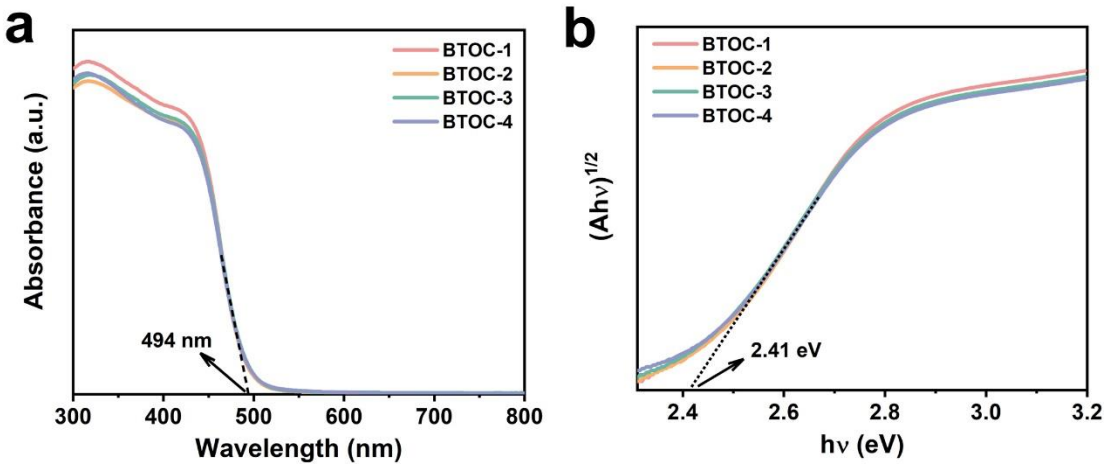

Fig. S6. (a) DRS spectra, and (b) corresponding Tauc plots of as-synthesized catalysts.

The optical properties and electronic band structures of the as-synthesized catalysts were systematically investigated. DRS profiles (Fig. S6a) reveal that the flux-mediated synthesis does not alter the fundamental light absorption characteristics of the materials. Tauc plot analysis (Fig. S6b) yields an identical band gap (Eg) of approximately 2.41 eV for all samples based on equation:[1]

$$\alpha h\nu = A(h\nu - E_g)^2$$

where α, h, ν, and A represent the absorption coefficient, Planck's constant, light frequency, and a constant, respectively.

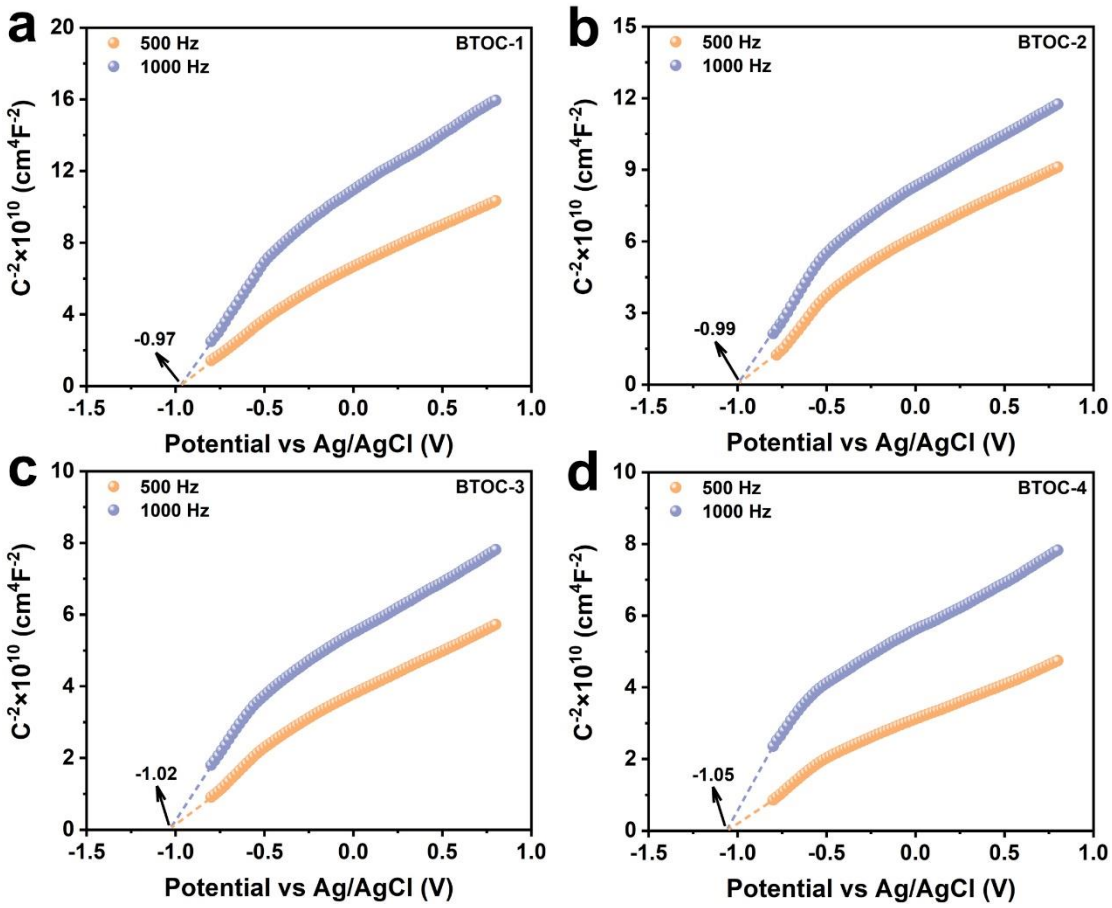

Fig. S7. Mott-Schottky plots of (a) BTOC-1, (b) BTOC-2, (c) BTOC-3, and (d) BTOC-4.

Mott-Schottky measurements (Fig. S7) were performed to determine the flat-band potentials (E_{FB}) of the catalysts.[2] The E_{FB} of BTOC-1 to BTOC-4, derived from the x-axis intercepts of the linear regions, were measured as -0.97, -0.99, -1.02, and -1.05 V vs. Ag/AgCl, respectively. These values correspond to -0.77, -0.79, -0.82, and -0.85 V relative to the normal hydrogen electrode (NHE) using the conversion $E_{(NHE)} = E_{(Ag/AgCl)} + 0.197$ V. The positive slopes of the plots unequivocally confirm the n-type semiconductor nature of all materials. Considering that the conduction band potential (E_{CB}) is approximately 0.2 V more negative than E_{FB}, the E_{CB} values are estimated to be -0.97, -0.99, -1.02, and -1.05 V (vs. NHE) for the corresponding samples. Consequently, their valence band potentials (E_{VB}) were calculated to be

+1.44, +1.42, +1.39, and +1.36 V (vs. NHE).

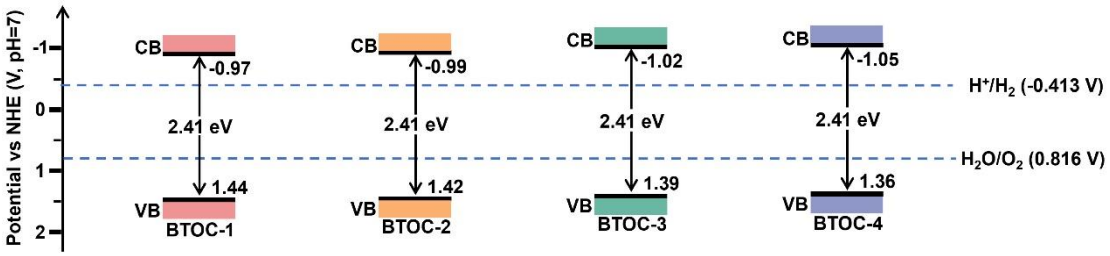

Fig. S8. The band structure of as-synthesized catalysts.

As schematically illustrated in Fig. S8, the conduction band potentials of all catalysts are sufficiently negative to thermodynamically drive proton reduction (H_2 evolution), and their E_{VB} levels are sufficiently positive to enable water oxidation (O_2 evolution).[3] Notably, from BTOC-1 to BTOC-4, a slight but consistent enhancement in reduction potential is accompanied by a gradual decrease in oxidation potential. This trend runs opposite to the observed H_2 and O_2 evolution activities, confirming that the slight modulation in the band structure is not the determinant of the altered photocatalytic redox preference.

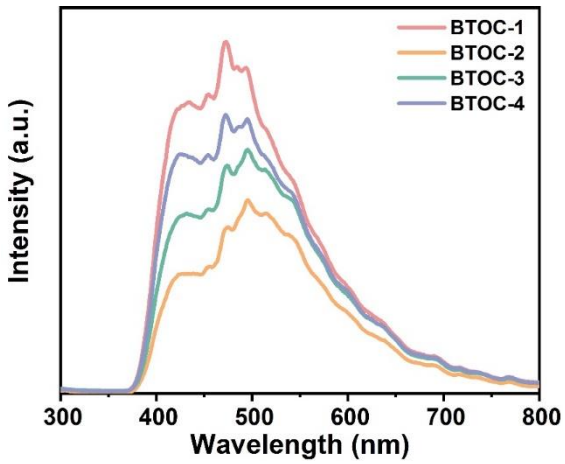

Fig. S9. PL spectra of as-fabricated samples.

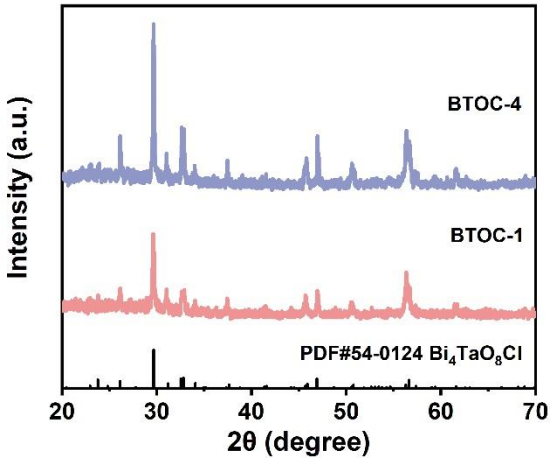

Fig. S10. XRD patterns of BTOC-1 and BTOC-4 after photocatalytic H_2 evolution for 1 h.

Table S1. The average geometric parameters of as-prepared samples acquired from SEM images.

Parameters	BTOC-1	BTOC-2	BTOC-3	BTOC-4
Length/nm	627	671	733	760
Width/nm	523	542	564	592
Thickness/nm	105	93	80	67
Area of (001)/nm^2	327921	363682	413412	449920
Area of (110)/nm^2	65835	62403	58640	50920
Area of (1$\bar{1}$0)/nm^2	54915	50406	45120	39664
{110}/{001} ratio	0.368	0.310	0.251	0.201
{001} exposure percentage	73.1%	76.3%	79.9%	83.2%

Note: For each sample, the length (L) and width (W) were determined by averaging measurements from 50-100 randomly selected nanoplates via SEM, while the thickness (T) was derived from 30-50 individual nanoplates. Assuming a rectangular prism geometry, the area of the (001) facet was calculated as L × W, whereas the areas of the (110) and (1$\bar{1}$0) facets were calculated as L × T and W × T, respectively. Given that the {110}-type family comprises four lateral facets and the {001}-type family consists of two basal planes, the {110}/{001} ratio and the {001} exposure percentage were subsequently calculated based on the corresponding total area ratio.

Table S2. Summary of the parameters for AQE test.

λ (nm)	P (mW/cm^2)	S (cm^2)	t (s)	H_2 (μmol)	AQE	O_2 (μmol)	AQE
420	204	24.63	3600	27.84	0.28%	16.39	0.32%
450	196			23.71	0.23%	13.18	0.25%
500	193			0	0%	0.69	0.01%
550	191			0	0%	0.36	0.01%

Table S3. Summary of the fitting parameters for the TR-PL decay curves of as-prepared catalysts.

Sample	Decay time (ns)		Amplitude (percentage)		$\tau_{Ave.}$ (ns)	R^2
	τ_1	τ_2	A_1 (I_1)	A_2 (I_2)		
BTOC-1	0.81	5.91	467.53 (90.29)	50.29 (9.71)	3.05	0.990
BTOC-2	0.83	6.41	461.07 (88.71)	58.70 (11.29)	3.59	0.990
BTOC-3	0.92	5.26	422.49 (81.80)	93.97 (18.20)	3.35	0.992
BTOC-4	0.76	3.93	410.96 (84.93)	72.90 (15.07)	2.28	0.992

The parameters were obtained by fitting decay curves using the equation:[4]

$$y=y_0+A_1\cdot e^{-\frac{t}{\tau_1}}+A_2\cdot e^{-\frac{t}{\tau_2}}$$

The average lifetime was calculated by using the equation:

$$\tau_{Ave.}=\frac{I_1\cdot\tau_1^2+I_2\cdot\tau_2^2}{I_1\cdot\tau_1+I_2\cdot\tau_2}$$

References

1. Z. Zhu, H. Huang, L. Liu, F. Chen, N. Tian, Y. Zhang and H. Yu, *Angew. Chem., Int. Ed.*, 2022, **61**, e202203519.
2. X. Zhang, C. Hu, Z. Zhu, Y. Zhang, S. Tu, Y. Zhang, T. Ma, F. Chen and H. Huang, *J. Colloid Interface Sci.*, 2023, **650**, 1536-1549.
3. J. Abdul Nasir, A. Munir, N. Ahmad, T. u. Haq, Z. Khan and Z. Rehman, *Adv. Mater.*, 2021, **33**, 2105195.
4. W. Yu, F. Chen, X. Zhang, N. Tian, N. Zhang, Y. Zhang and H. Huang, *Nano Energy*, 2025, **138**, 110862.